COMPENSATION OF PHASE ERROR CAUSED BY GROUND HEIGHT AMONG POLARIMETRIC CHANNELS IN X-BAND Pi-SAR

Toshifumi Moriyama, Makoto Satake, Seiho Uratsuka, Toshihiko Umehara,
Akitsugu Nadai, Takeshi Matsuoka and Kazuki Nakamura
National Institute of Information and Communications Technology (NICT)
4-2-1 Nukui-kita, Koganei-shi, Tokyo 184-8795 Japan
E-mail toshi.moriyama@nict.go.jp

1. Introduction

This paper discusses a compensation technique of phase error among polarimetric channels in the X-band Pi-SAR. Pi-SAR which has two synthetic aperture radar (SAR) systems of L-band and X-band was developed by CRL (now NICT) and NASDA (now JAXA), and can observe wide area with a high resolution in polarimetry mode. In addition, X-band system has a cross-track interferometry mode. Therefore, the observation targets of Pi-SAR may include various areas such as ocean, glacier, polar ice, forest, desert, mountain, urban area and so on. However, a problem of polarimetric calibration occurs in X-band Pi-SAR when polarimetric analysis for a mountain area in standard polarimetric data is examined. This problem is caused by the phase error among polarimetric channels related to ground height, because there is a separation between Horizontal (H) polarization and Vertical (V) polarization antenna locations in the elevation direction. In this paper, we attempt a compensation for the phase error of X-band Pi-SAR by using the interferometric data which can be simultaneously acquired with the polarimetric data.

2. Polarimetric calibration method

In order to perform a polarimetric calibration of POLSAR data, a polarimetric calibration model is needed physically and mathematically. A system block diagram of polarimetric imaging radar and a photograph of antenna used by X-band Pi-SAR are shown in Fig. 1 and 2. The feature of X-band Pi-SAR configuration is a separation between H pol. and V pol. antenna locations in elevation direction. For physical calibration model, the six paths for dual polarization waves can be considered in this POLSAR system (as shown in Fig. 1). The each contribution of six paths with respect to amplitude and phase is given as,

$$\begin{aligned}&\text{Path 1: } A_H^{Tr.} = \left|A_H^{Tr.}\right|\exp(j\phi_H^{Tr.}),\ \text{Path 2: } A_V^{Tr.} = \left|A_V^{Tr.}\right|\exp(j\phi_V^{Tr.}),\quad \text{Path 3: } A_H = \exp(j\phi_H),\\ &\text{Path 4: } A_V = \exp(j\phi_V),\qquad \text{Path 5: } A_H^{Rec.} = \left|A_H^{Rec.}\right|\exp(j\phi_H^{Rec.}),\ \text{Path 6: } A_V^{Rec.} = \left|A_V^{Rec.}\right|\exp(j\phi_V^{Rec.}),\end{aligned} \quad (1)$$

where we assume that the effects of amplitude for path 3 and path 4 are neglected, because they are compensated by a radiometric calibration in synthetic aperture processing. These six contributions influence a element of the measured scattering matrix $\boldsymbol{Z}$.

$$\begin{aligned}Z_{HH} &= A_H^{Rec.} A_H S_{HH} A_H A_H^{Tr.}, \qquad Z_{HV} = A_H^{Rec.} A_H S_{HV} A_V A_V^{Tr.},\\ Z_{VH} &= A_V^{Rec.} A_V S_{VH} A_H A_H^{Tr.}, \qquad Z_{VV} = A_V^{Rec.} A_V S_{VV} A_V A_V^{Tr.}.\end{aligned} \quad (2)$$

If eq. (2) is normalized by $A_H^{Rec.} A_H A_H A_H^{Tr.}$, the simple form of eq. (2) can be derived as,

$$Z'_{HH} = S_{HH},\ Z'_{HV} = F_2 S_{HV},\ Z'_{VH} = F_1 S_{VH},\ Z'_{VV} = F_1 F_2 S_{VV}, \quad (3)$$

$$\begin{aligned}F_1 &= \left|A_V^{Rec.}/A_H^{Rec.}\right|\exp\left\{-j\left(\phi_V^{Rec.} - \phi_H^{Rec.}\right)\right\}\exp\left\{-j\left(\phi_V - \phi_H\right)\right\} = f_1\exp\left\{-j\left(\phi_V - \phi_H\right)\right\},\\ F_2 &= \left|A_V^{Tr.}/A_H^{Tr.}\right|\exp\left\{-j\left(\phi_V^{Tr.} - \phi_H^{Tr.}\right)\right\}\exp\left\{-j\left(\phi_V - \phi_H\right)\right\} = f_2\exp\left\{-j\left(\phi_V - \phi_H\right)\right\}.\end{aligned} \quad (4)$$

On the other hand, for mathematical polarimetric calibration model, the system effects of POLSAR was modeled by a two-stage linear process, and the measured scattering matrix $\boldsymbol{Z}$ can be written as,

$$\boldsymbol{Z} = \boldsymbol{RST} + \boldsymbol{N}, \qquad \boldsymbol{R} = \begin{pmatrix}1 & \delta_1\\ \delta_2 & f_1\end{pmatrix}, \qquad \boldsymbol{T} = \begin{pmatrix}1 & \delta_3\\ \delta_4 & f_2\end{pmatrix}, \quad (5)$$

ISBN: 89-86522-78-0 94460©KEES

where $\boldsymbol{R}$ and $\boldsymbol{T}$ are 2x2 complex matrices describing the phase and amplitude distortions related to receiver and transmitter, respectively, and $\boldsymbol{N}$ is noise. Moreover, $f_{i=1,2}$ and $\delta_{i=1,2,3,4}$ mean H/V imbalance and cross-talk. If cross-talk and noise are close to zero, eq. (5) can be approximated as eq. (3) except for the term of $\exp\{-j(\phi_V - \phi_H)\}$. The $\exp\{-j(\phi_V - \phi_H)\}$ depends on a separation between antenna locations. Thus, the physical model shown in Fig. 1 can be related to the mathematical model expressed by eq. (5).

In general, the polarimetric calibration parameters ($f_{i=1,2}$ and $\delta_{i=1,2,3,4}$) are estimated by using a trihedral corner reflector and the distributed targets which satisfy a property of the reflection symmetry. However, this calibration technique is insufficient to support a calibration of X-band Pi-SAR, since the phase of F_1 and F_2 varies with slant range distance due to ($\phi_V - \phi_H$). An element of scattering matrix calibrated by Van Zyl's method [2] or Quegan's method [3] is given as,

$$\begin{aligned} S'_{HH} &= S_{HH}\,, & S'_{HV} &= S_{HV}\exp\{-j(\phi_V - \phi_H)\}\,, \\ S'_{VH} &= S_{VH}\exp\{-j(\phi_V - \phi_H)\}\,, & S'_{VV} &= S_{VV}\exp\{-j2(\phi_V - \phi_H)\}\,. \end{aligned} \tag{6}$$

Therefore, a polarimetric calibration of X-band Pi-SAR needs to compensate not only the system error (f and δ) but also the phase error with respect to $\phi_V - \phi_H$ among polarimetric channels.

3. Compensation method of phase error

The phase error ($\phi_V - \phi_H$) among polarimetric channels is caused by a space between H pol. and V pol. antenna locations in elevation direction. On the other hand, this phase error can be esimated as the phase difference between master and slave antennas in the interferometric observation. Thus, the key point to compensate phase error among polarimetric channels of X-band Pi-SAR is that the interferometric data which can be obtained with polarimetric data simultaneously is used. In X-band Pi-SAR system, using the geometry of Fig. 3, the phase difference of polarimetric and interferometric observation modes becomes,

$$\text{Polarimetry mode :} \quad \phi_V - \phi_H = (4\pi B_P/\lambda)\sin(\theta_P - \theta), \tag{7a}$$

$$\text{Interferometry mode :} \quad \phi_M - \phi_S = (2\pi B_I/\lambda)\sin(\theta - \theta_I), \tag{7b}$$

where $B_{n=I,P}$ and $\theta_{n=I,P}$ are length and tilt angle of a baseline, respectively, θ is a local incident angle, and λ is the wave length. Then, the polarimetry mode can be connected to the interferometry mode by local incident angle θ. In addition, the phase difference of eq. (7) can be divided into two terms of ground range distance and ground height. To compensate the contribution of ground range distance that had already been reported [4] is relatively easy. In this paper, the term of ground height is considered. The phase difference by ground height can be extracted from eq. (7) as,

$$\text{Polarimetry mode :} \quad (\phi_V - \phi_H)_{ground\ height} \approx (4\pi B_P/\lambda)\cos(\theta_P - \theta_0)(\theta_0 - \theta), \tag{8a}$$

$$\text{Interferometry mode :} \quad (\phi_M - \phi_S)_{ground\ height} \approx (2\pi B_I/\lambda)\cos(\theta_I - \theta_0)(\theta - \theta_0), \tag{8b}$$

where θ_0 is an incident angle to the reference flat surface. Since the phase difference $(\phi_V - \phi_H)_{\text{ground height}}$ is influenced by various polarimetric scattering effects (such as double-bounce scattering, shift of scattering center among polarimetric channels, etc), θ cannot be retrieved from POLSAR data. However, we can estimate θ and $(\phi_V - \phi_H)_{\text{ground height}}$ from the interferometry data. Therefore, the compensated polarimetric data are obtained from a multiplication of $\exp\{j(\phi_V - \phi_H)\}_{\text{ground height}}$ estimated by the interferometry data as follows:

$$\begin{aligned} S_{HH} &= S'_{HH}\,, & S_{HV} &= S'_{HV}\exp\{j(\phi_V - \phi_H)_{ground\ height}\}, \\ S_{VH} &= S'_{VH}\exp\{j(\phi_V - \phi_H)_{ground\ height}\}, & S_{VV} &= S'_{VV}\exp\{j2(\phi_V - \phi_H)_{ground\ height}\}. \end{aligned} \tag{9}$$

4. Compensation results

In order to confirm a usefulness of above-mentioned compensation technique for X-band

Pi-SAR, the POLSAR data acquired over Mt. Kaimondake, Kagoshima, on February 7, 2004 is used. The color composite image (HH: Red, HV: Green, VV: Blue) of X-band Pi-SAR is shown in Fig. 4 and its size is 5km by 5km. A ground height at the top of Mt. Kaimondake is 922m above see level. Figure 5 shows the phase difference image between HH and VV in X-band. Note that the contribution of ground range distance is subtracted in this phase data. The change of phase from $-\pi$ to π with respect to ground height appears in this image. Using phase difference data of polarimetry data and interferometry data, we calculated a ground height profile (shown in Fig. 6) corresponding to the marked range line in Fig. 4. There is a fluctuation in polarimetry profile due to small baseline length (which is about 20cm) and the effect of double-bounce scattering. However, these two ground height profiles agree roughly. Therefore, there is a possibility that the interferometric data can compensate the phase error of polarimetric data in X-band Pi-SAR. An example of the compensation of phase error is shown in Fig. 7, where we indicate averaged alpha image before and after compensation based on the ground height derived from interferometric data. In an uncompensated averaged alpha image, the scattering mechanism in the mountain area is estimated as a double bounce scattering (which is indicated by the red). Since the double bounce scattering does not arise in the area on a mountain side due to slope of ground surface, this result is inconsistent with the physical phenomenon. On the other hand, the image after compensation dose not show the contribution of the double bounce scattering.

5. Conclusion

The compensation method of phase error among polarimetric channels is presented for X-band Pi-SAR. This phase error is caused by a separation between H pol. and V pol. antenna locations in elevation direction, and varies with a change of ground height. Since the mechanism of the phase error is similar to the principle of interferomery, the interferometry data which can be acquired with the polarimetric data is used for compensation. The compensation result shows the applicability of polarimetric analysis to the data of a mountain area obtained by X-band Pi-SAR.

References

[1] T. Kobayashi, T. Umehara, et al, "Airborne Dual-Frequency Polarimetric and Interferometric SAR," IEICE Trans. Commun., vol.E83-B, no.9, pp.1945-1954, Sep. 2000.

[2] J. J. van Zyl, "Calibration of Polarimetric Radar Images Using Only Image Parameters and Trihedral Corner Reflectors," IEEE Trans. Geosci. Remote Sensing, vol.28, no.3, pp.337-348, May 1990.

[3] S. Quegan, "A Unified Algorithm for Phase and Cross-Talk Calibration of Polarimetric Data-Theory and Observation," IEEE Trans. Geosci. Remote Sensing, vol.32, no.1, pp.89-99, Jan. 1994.

[4] M. Satake, T. Umehara, H. Maeno, S. Uratsuka and H. Nakayama, "Range Antenna Pattern Measurement of Airborne SAR System with Arrayed Corner Reflectors," Proc. of International Geoscience and Remote Sensing Symposium 2002 (IGARSS), No.03-09-12, pp.859-861, June 2002.

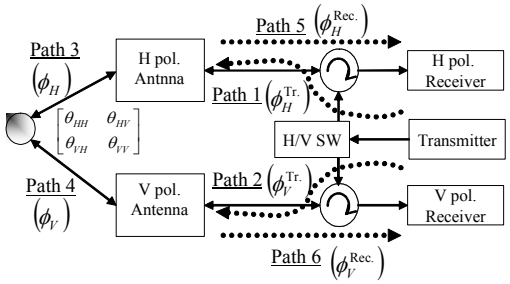

Fig.1 System block diagram of polarimetric imaging radar.

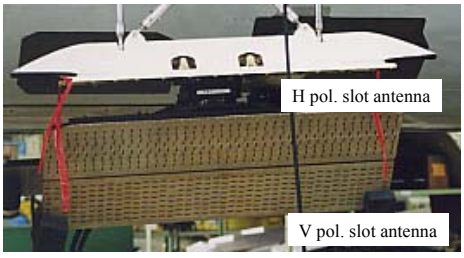

Fig.2 Photograph of antenna used by X-band Pi-SAR.

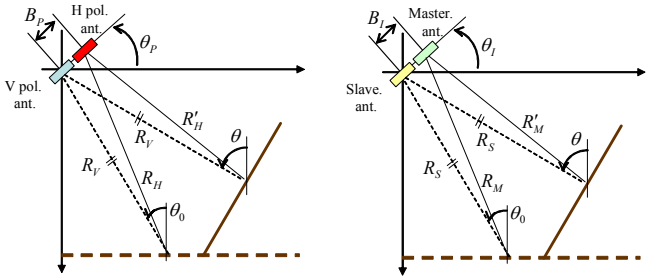

Fig.3 Geometry of two observation modes.
(a) Polarimetry mode. (b) Interferometry mode.

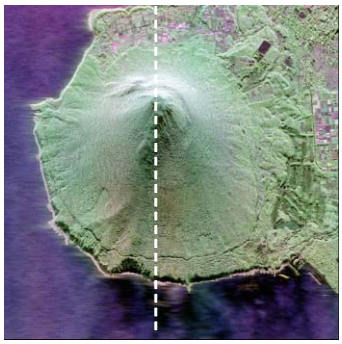

Fig.4 Color composite image of Mt. Kaimondake.

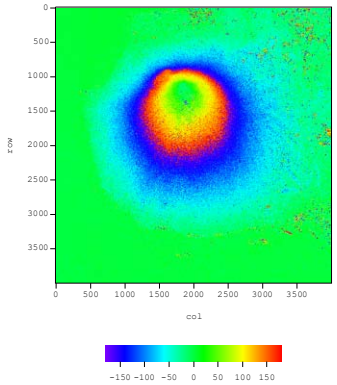

Fig.5 Phase difference image between HH and VV.

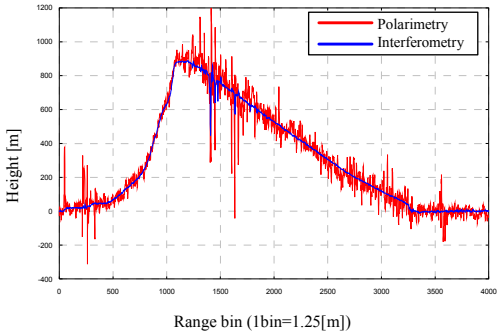

Fig.6. Height profile corresponding to the marked range line in Fig.3.

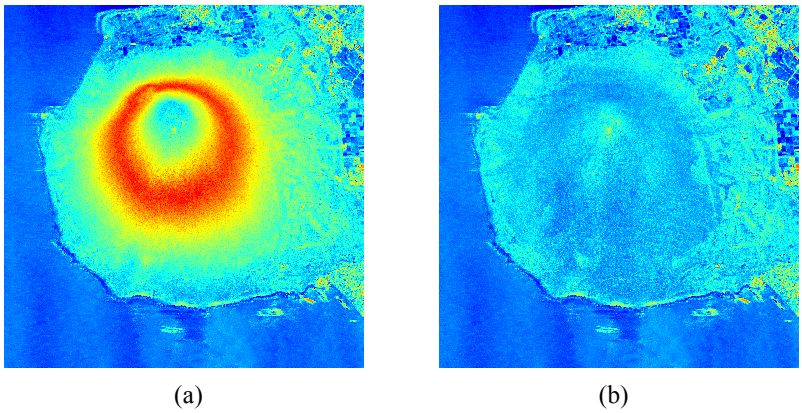

(a) (b)

Fig.7 Averaged alpha image. (a) Before compensation. (b) After compensation.